Atomic-Scale Force-Vector Fields

Kai Ruschmeier and André Schirmeisen*

Center for Nanotechnology (CeNTech), Heisenbergstrasse 11, 48149 Münster, Germany
Physikalisches Institut, Westfälische Wilhelms-Universität Münster, Wilhelm-Klemm-Strasse 10, 48149 Münster, Germany

Regina Hoffmann

Physikalisches Institut and DFG-Center for Functional Nanostructures, Universität Karlsruhe, 76128 Karlsruhe, Germany
(Received 20 March 2008; published 7 October 2008)

The magnitude and direction of forces acting between individual atoms as a function of their relative position can be described by atomic-scale force-vector fields. We present a noncontact atomic force microscopy based determination of the force fields between an atomically sharp tip and the (001) surface of a KBr crystal in conjunction with atomistic simulations. The direct overlap of experiment and simulation allows identification of the frontmost tip atom and of the surface sublattices. Superposition of vertical and lateral forces reveals the spatial orientation of the interatomic force vectors.

DOI: 10.1103/PhysRevLett.101.156102 PACS numbers: 68.37.Ps, 07.79.Lh, 87.64.Dz

Using an atomic force microscope (AFM) [1], one can measure interatomic forces either while the tip is scanned in a direction parallel to a surface (imaging) or while the tip is approached and retracted from the sample surface [2] (force distance curves). Dynamic modes where the tip is oscillated have allowed both true atomic resolution during imaging [3] and tip-sample forces of the atomic lattice at specific sites [4,5] to be obtained. This ability has culminated in the chemical identification of surface atoms [5–7]. Further, a systematic acquisition of adjacent force distance curves allows one to determine three-dimensional atomic force fields above the sample surface [8,9].

The recent growing interest [10–13] in the force field technique stems from several aspects. On one hand, three-dimensional atomic-scale force fields facilitate assessing lateral relaxations of the tip-sample contact occurring during the approach as well as experimental artifacts such as piezoelectric drift. On the other hand, acquisition of the vertical force field allows one to calculate the potential energy barriers [10] and landscapes [13]. Moreover, this technique gives direct access to lateral atomic forces [9,11], which have been exploited to determine the lateral force needed to move an atom on a surface [13].

From a superposition of the simultaneously measured vertical and lateral atomic force fields in AFM experiments, one can construct a vector field. This force-vector field thus represents the magnitude and direction of forces acting between the terminating tip apex atom and the surface atoms. However, for a sound understanding of the underlying atomic processes, a direct evaluation of experiments in conjunction with atomistic simulations is necessary. Here we present a concerted analysis of experimental force-vector fields from noncontact AFM measurements on KBr with theoretical simulations.

Measurements were carried out with an ultrahigh vacuum atomic force microscope (Omicron VT-AFM) at a base pressure below $p = 5 \times 10^{-10}$ mbar in frequency modulation mode. The excitation and frequency detection was performed by a Nanonis oscillation controller. As force sensors, commercial silicon tips were used (NCHR-SSS type, Nanosensors) with resonance frequency $f_0 =$ 289 549 Hz, spring constant $k = 20.4$ N/m, effective quality factor $Q = 9700$, and a nominal tip apex radius of 2 nm, driven at an oscillation amplitude of $A =$ 6.4($\pm$1.0) nm. The tip was sputtered twice (for 180 and 120 s) *in situ* with 500 eV Ar ions at a current of 7 μA to remove possible contaminations, while the amorphous silicon oxide at the tip apex is not completely removed. The KBr(001) sample was cleaved *in situ* and heated to 420 K for 60 min to equilibrate residual charges.

Initial surface scans showed atomic corrugation, but after an accidental tip crash the contrast was significantly improved, yielding images with single atomic defects before and after the spectroscopy experiments were performed. An example of an atomically resolved area of 2×2 nm^2 on the KBr (001) surface is shown in Fig. 1(a). To obtain the vertical force field, the frequency shift was

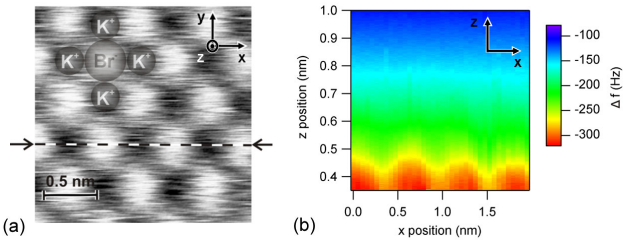

FIG. 1 (color online). (a) Surface topography of a KBr(001) sample, indicating the position of K^+ and Br^- surface ions according to the force field analysis. The dashed line indicates a representative y position along the sites of topography maxima at which the force field measurements were performed. (b) Measured frequency shift versus relative tip-sample distance (38 curves) as a function of the horizontal tip position along the x axis.

measured as a function of the relative tip-sample distance on a grid of 38 equally spaced points in the x direction and 6 equidistant positions in the y direction. Before and after each individual frequency shift versus distance measurement, the feedback loop was switched on to stabilize the system at a reference tip-sample distance for 104 ms. The frequency shift was measured over a range of 1.1925 nm in steps of 0.0025 nm, with a time constant of 5.12 ms for each data point. Together with the time needed for feedback stabilization, this resulted in a total acquisition time of 1.7 min per x-z slice. Additional frequency shift curves over a larger distance range (4.5 nm) were taken at several surface positions, in order to quantify the long range part of the tip-sample interaction. All measurements were performed at room temperature, which requires fast measurements with respect to drift rates. Positional drift was ≈ 0.001 nm/s, which is negligible in the z direction, since the z feedback is enabled every 2.44 s. In the lateral direction, this drift amounts to an uncertainty of 0.1 nm in the y position of a slice.

A two-dimensional color-coded map shows the unprocessed frequency-distance data as a function of lateral and vertical tip position along the corrugation maxima [Fig. 1(b)]. We have calculated the tip-sample forces from the frequency shift using the method described in Ref. [14]. The individual force curves in Fig. 2(a) contain the site-specific forces, responsible for the atomic-scale image contrast, as well as site-independent long range forces. The latter could be a superposition of van der Waals and electrostatic forces, whereas the site-specific part is dominated by short range chemical binding forces. Since in this work we focus on the site-specific forces it is necessary to separate the long range force interaction from the total tip-sample forces, assuming additivity of the different force contributions as a first-order approximation [4].

The long range part of the experimental forces [inset of Fig. 2(a)] has been fitted with a van der Waals law [15] for a conical tip with a spherical cap (solid gray line, Hamaker constant of $H = 6.5 \times 10^{-20}$ J [16]). The best fit was achieved with a cone angle of $\alpha = 20°$ and a tip radius of $r = 8.5$ nm in the range of $z = 1.1$–4.5 nm. The tip radius is larger than the specification given by the manufacturer ($r = 2$ nm), possibly due to soft tip-sample contacts performed before the experiments. These soft contacts will most likely lead to KBr-cluster termination at the tip apex, as assumed before [5,17,18]. In the short distance regime of $z < 1.1$ nm, the van der Waals fit underestimates the measured forces. This can have two reasons: The last several nanometers of the tip structure will be more complex than the simple model suggests. Second, there may be a background of electrostatic forces stemming from residual charges, which are not site-specific [17].

The forces on different lattice sites labeled A–D along a line between the two ionic species in Fig. 2(a) match within the noise up to $z = 0.62$ nm, while site-specific differences

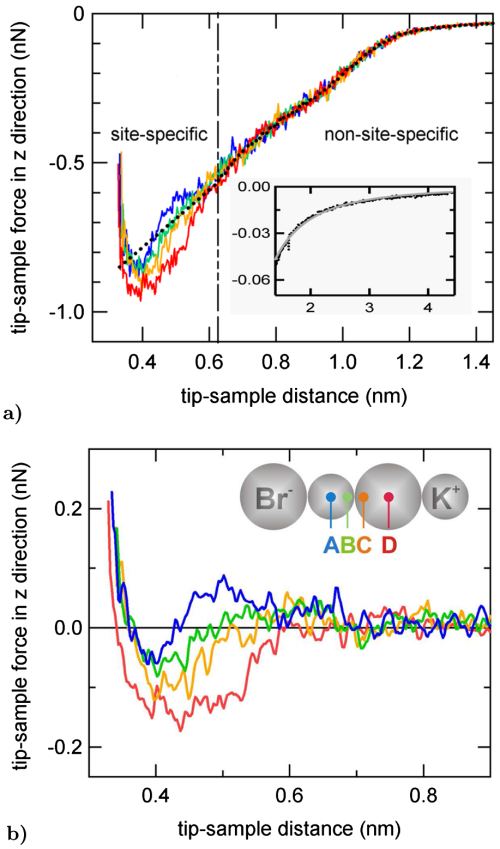

FIG. 2 (color online). (a) Experimental force curves at positions A–D along a line between the two ionic species. The black dotted curve represents the average over all force curves with a linear extrapolation into the regime of site-specific behavior. Inset: Solid gray curve is a van der Waals fit of the long range part of the force curves. (b) Site-specific part of the short range regime for the same force curves as in (a), where the non-site-specific contributions have been subtracted.

occur in the range $0.30 \text{ nm} < z < 0.62$ nm. In order to separate the site-specific from the long range forces, we are trying to approximate the non-site-specific force contribution for $z < 0.62$ nm, since in our case it is not possible to measure the long range forces only [4]. Alternatively, one could define one curve as a reference and subtract this from the force field. While this would eliminate the long range force part, the site-specific part of the reference curve would be superimposed on all other force curves. The precise long range force law is unknown; however, we find that the forces in the non-site-specific regime are sufficiently well approximated by a line fit for $0.62 \text{ nm} < z < 1.10$ nm, which can be extrapolated into the site-specific regime. This first-order approximation is justified, since any long range background force is expected to show a continuous curve shape and should not contribute to atomic-scale features. Figure 2(b) shows the resulting short range contribution of the experimental force curves.

The corresponding site-specific vertical force field is illustrated in Fig. 3(a), which is based on 23 adjacent force curves. The red areas of attractive forces up to

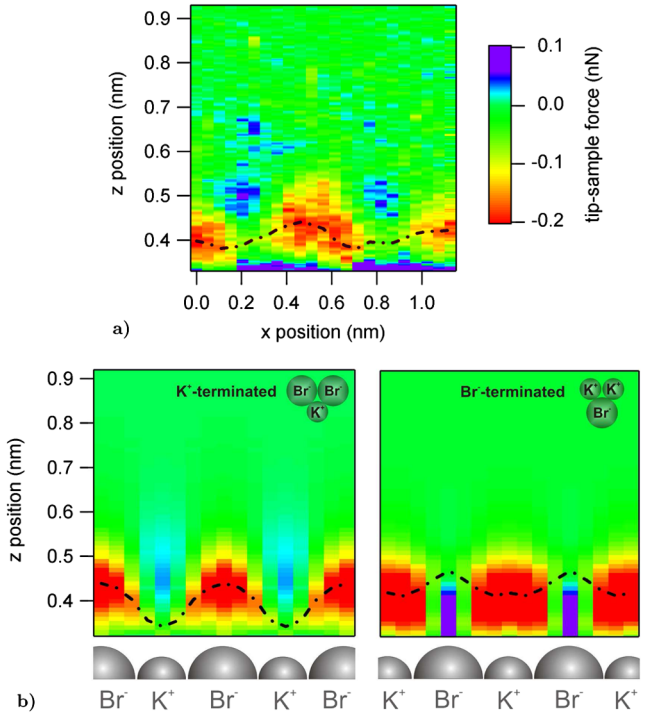

FIG. 3 (color online). (a) The two-dimensional map of the site-specific vertical tip-sample forces. (b) Simulated map of the site-specific tip-sample forces for a K^+-terminated KBr-cluster (left) and for a Br^--terminated KBr cluster (right). The dotted black lines indicate the minimum of the force curves with respect to the z axis at each x position.

$F = -0.18$ nN at the x position of one ionic species on the surface show a roughly triangular shape in the force map. In between the attractive force areas, we find blue circularly shaped areas with repulsive forces up to $F = 0.07$ nN around $z = 0.50$ nm at the location of the oppositely charged surface ion.

In order to compare our measurements with calculations, our tip-sample system was simulated using the code SCIFI [5,19]. The sample consisted of a system of 6 layers of 10×10 ions of which the bottom layer and the sides where kept fixed. A $(KBr)_{32}$ cluster was taken as the tip with the $\langle 111 \rangle$ direction perpendicular to the sample surface. In this orientation, the cluster contains 10 layers of equally charged ions. The frontmost five atomic layers of the tip were allowed to relax. Atomistic interactions were represented by suitable Buckingham potentials taken from Ref. [20].

Calculations were performed for two different tip configurations: A K^+-ion-terminated and a Br^--ion-terminated tip cluster. The simulations were performed for both tip configurations at evenly spaced positions ($\Delta x = 0.08$ nm) between two neighboring K^+ and Br^- ions. Along the tip-sample distance axis, forces were calculated every 0.01 nm. In order to take the polarizability of the ions into account, a linear force acting between ion cores and shells was used [21]. In order to compute the resulting forces, the mechanical equilibrium coordinates for the shells and cores and the corresponding forces on the fixed tip ions were determined. Since the total charge of both the tip and the sample was zero, the resulting forces are short ranged; i.e., they decay within less than 1 nm distance from the surface. Vertical and lateral tip apex ion relaxations were less than 40 pm in all calculations, whereas the surface Br^- ion moved less than 50 pm when the K^+-terminated tip was approached.

Figure 3(b) shows the simulated short range force fields for both tips, each starting in the x direction with the tip approaching the oppositely charged ion, e.g., a K^+-terminated tip above a Br^- sample ion. Significant differences in the behavior of the tip-sample forces for the two tip configurations manifest, on one hand, in the shape of the spots of maximum attractive forces, which show a triangular shape for the K^+-terminated tip, whereas the Br^- tip exhibits a square structure. More prominently, the repulsive forces have different characteristics: For the K^+ tip approaching the same charged K^+ surface ion, a local repulsive force maximum is observed at distances around $z = 0.45$ nm, before the onset of strongly repulsive forces occurs at $z < 0.35$ nm. In contrast, repulsive electrostatic forces for the Br^- tip approaching the Br^- surface ion already appear at $z < 0.43$ nm and stay repulsive until the minimum distance considered here. These results do not significantly change if the tip cluster is rotated with respect to its [111] axis which points in the direction perpendicular to the sample surface [5]. Note that similar results have been obtained using density functional theory methods [18].

Direct comparison of the experimental and simulated force maps in Fig. 3 shows excellent agreement for the case of the K^+-terminated tip. On one hand, the position and shape of the weakly repulsive regime (blue areas) as well as the triangular shaped attractive force regime (red areas) in Fig. 3(a) are well reproduced by the simulated force map at the left-hand side of Fig. 3(b). A characteristic difference between the K^+- and Br^+-terminated tips is reflected in the course of the minima in the force curves with respect to the z axis (dotted black lines), showing the opposite trend for the two tips. This trend is independent of the subtracted long range force law. Again, comparison with the experiment shows agreement with the assumption of a K^+-terminated tip.

Furthermore, we find quantitative agreement for the forces at different sites. In order to be independent of possible offsets, we calculate the difference between the maximum and minimum values along a force distance curve, which for site A is 0.118 ± 0.080 nN and for site D is 0.198 ± 0.073 nN. The corresponding values in the simulations for the K^+ tip show good agreement (0.119 and 0.267 nN, respectively), whereas systematic discrepancies are found for the Br^- tip (0.029 and 0.346 nN). Thus, we conclude that the experimental force fields were measured with a K^+-terminated tip apex, while the exact geometry of the rest of the tip apex atoms may still be different in experiment and simulation.

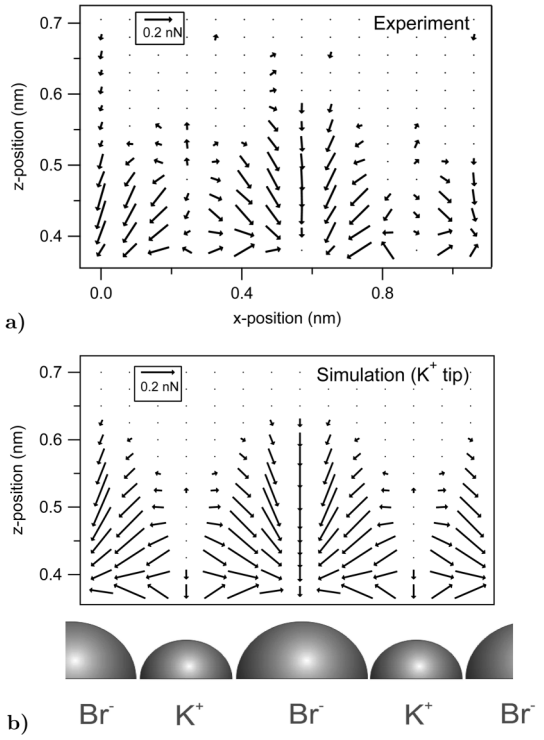

FIG. 4. (a) Atomic-scale force-vector field on KBr(001) determined from the AFM experiment. Arrow length and orientation represent magnitude and direction, respectively, of the site-specific force experienced by the tip at the respective position in the x-z plane. (b) Simulated force-vector field for the K-terminated tip apex. Length scales for the vectors are indicated in the upper left corners.

We proceed by calculating the lateral tip-sample forces from the force fields by integration in the z direction and subsequent differentiation in the x direction [9,11]. Combining the vertical and lateral forces allows us to extract the corresponding force vectors in the x-z plane. Those vectors quantify magnitude and direction of the site-specific force experienced by an atomically sharp tip at the respective position in the x-z plane above the surface. Figures 4(a) and 4(b) show the resulting experimental and simulated (K^+ termination) force-vector fields. Apart from a slight asymmetry in the vector fields at very small z distances, which might be due to asymmetric lateral tip atom relaxations, good agreement between experiment and calculations is found. The force-vector maps show that approaching the tip directly above a K^+ ion leads to no lateral forces, whereas the lateral forces are strongest at the position between the K^+ and Br^- sample ions, always pointing towards the Br^- ion. This is a consequence of the local energy minima at the Br^- sites. The observed lateral forces of about 0.2 nN [22] are comparable to lateral forces during atom manipulation [13] as well as atomic friction studies [23].

Our results present a direct comparison of atomic-scale force-vector fields from experiments with simulations on KBr surfaces. The qualitative and quantitative agreement shows that the simulation captures all essential elements of the experiment, in particular, validating the assumption that a cluster of the surface material is responsible for the observed image contrast, despite the fact that the atomistic details of the tip cluster remain unknown.

Discussions and support by Harald Fuchs and Hendrik Hölscher are gratefully acknowledged, as well as financial support by the DFG (SCHI619/1-2 and TRR 61 Project No. B7). R. H. acknowledges financial support of the Landesstiftung Baden-Württemberg.

*schirmeisen@uni-muenster.de

[1] G. Binnig, C. F. Quate, and C. Gerber, Phys. Rev. Lett. **56**, 930 (1986).
[2] S. P. Jarvis *et al.*, Nature (London) **384**, 247 (1996).
[3] F.-J. Giessibl, Science **267**, 68 (1995).
[4] M. A. Lantz *et al.*, Science **291**, 2580 (2001).
[5] R. Hoffmann *et al.*, Phys. Rev. Lett. **92**, 146103 (2004).
[6] A. S. Foster, C. Barth, A. L. Shluger, and M. Reichling, Phys. Rev. Lett. **86**, 2373 (2001).
[7] Y. Sugimoto *et al.*, Nature (London) **446**, 64 (2007).
[8] H. Hölscher, S. M. Langkat, A. Schwarz, and R. Wiesendanger, Appl. Phys. Lett. **81**, 4428 (2002).
[9] A. Schwarz, H. Hölscher, S. M. Langkat, and R. Wiesendanger, in *Scanning Tunneling Microscopy/Spectroscopy and Related Techniques*, AIP Conf. Proc. No. 696 (AIP, New York, 2003), p. 68.
[10] A. Schirmeisen, D. Weiner, and H. Fuchs, Phys. Rev. Lett. **97**, 136101 (2006).
[11] M. Abe *et al.*, Appl. Phys. Lett. **90**, 203103 (2007).
[12] M. Heyde, G. H. Simon, H.-P. Rust, and H.-J. Freund, Appl. Phys. Lett. **89**, 263107 (2006).
[13] M. Ternes *et al.*, Science **319**, 1066 (2008).
[14] U. Dürig, Appl. Phys. Lett. **75**, 433 (1999).
[15] M. Guggisberg *et al.*, Phys. Rev. B **61**, 11 151 (2000).
[16] R. Hoffmann *et al.*, Appl. Surf. Sci. **188**, 238 (2002).
[17] M. A. Lantz *et al.*, Phys. Rev. B **74**, 245426 (2006).
[18] O. H. Pakarinen *et al.*, Phys. Rev. B **73**, 235428 (2006).
[19] L. N. Kantorovich and A. S. Foster, SCIFI v1.0 Manual 1.3.2000.
[20] M. J. L Sangster and R. M. Atwood, J. Phys. C **11**, 1541 (1978).
[21] The polarizability α of the material, defined by the dependence of the dipole moment $\vec{p}$ of each ion $\vec{p} = \alpha\vec{E}$ on the local electrostatic field $\vec{E}$ generated by the other ions, is modeled by a linear force with a spring constant $c = Q^2/(4\pi\epsilon_0\alpha)$, where Q is the shell charge.
[22] Lateral tip stiffness was estimated by a finite element simulation to be $c_{\text{lateral}} = 8.8\ \text{N/m}$, thus leading to tip relaxations below 30 pm for the observed forces.
[23] A. Socoliuc, R. Bennewitz, E. Gnecco, and E. Meyer, Phys. Rev. Lett. **92**, 134301 (2004).